

Research Article

Effect of Magnetic Field Coupled Deep Cryogenic Treatment on Wear Resistance of AISI 4140 Steel

Liang Tang, Xianguo Yan , Yijiang Jiang, Fan Li, and Haidong Zhang

School of Mechanical Engineering, Taiyuan University of Science and Technology, Taiyuan 030024, China

Correspondence should be addressed to Xianguo Yan; yan_xg2008@126.com

Received 5 December 2019; Accepted 18 February 2020; Published 30 March 2020

Academic Editor: Guru P. Dinda

Copyright © 2020 Liang Tang et al. This is an open access article distributed under the Creative Commons Attribution License, which permits unrestricted use, distribution, and reproduction in any medium, provided the original work is properly cited.

In this study, a new magnetic field coupled deep cryogenic treatment (MDCT) is developed and its effect on wear resistance of AISI 4140 steel is investigated. Compared with wear resistance of untreated (UT), wear resistance of MDCT increases by 29%. Wear resistance is inversely proportional to the friction coefficient. The treatment promotes the phase transformation and dislocation movement to generate more martensite in multidirectional distribution and optimized carbide. It enhances material property and repairs surface defect. Moreover, the wear mechanism of MDCT is only abrasive wear in the form of microscopic cutting, while other process groups are oxidative wear and abrasive wear in the form of microscopic cutting and microscopic fracture.

1. Introduction

Conical pick is a cutting tool that is widely used in mining coal. It is composed of cemented carbide tip embedded in alloy steel body. Due to excellent mechanical property and low cost, the AISI 4140 steel is often selected as the pick body material. However, wear resistance of this material is still lower than cemented carbide tip. Under the complicated working condition, the pick body is most likely to cause wear failure [1]. It leads to the pick tip falloff and directly affects efficiency of the coal mining machine (Figure 1). Therefore, it is especially necessary to improve the wear resistance of material. Wear resistance is often related to structure design, material choice, and process treatment. Among them, process treatment is a convenient and effective measure.

Cryogenic treatment is an efficient method to enhance the materials property and the service life, which has been widely recognized by scholars [2–5]. The principle of cryogenic treatment is to lower the temperature of the material to the ultralow temperature state. The low temperature environment strengthens the material to improve performance [6, 7]. Cryogenic treatment has a very early research history. In the 1930s and 1940s, many researchers began to explore the effect of low temperature treatment on

the property of high-speed steel T1 [8–10]. The process is then gradually extended to other materials. The grinding wear performance of cryotreated Cr-Mn-Cu alloy iron is better than that of conventionally destabilized [11]. For AISI 4140 steel, the paper obtains optimal level of the cryogenic treatment process parameters and improves the wear resistance of the material [12].

In addition to cryogenic treatment, scholars magnetize material with ferromagnetism to enhance the material property [13–16]. There are two ways to apply magnetic field. The first way is to test performance after magnetic field treatment. Ma [17] investigates mechanical property changing mechanism of high-speed steel by pulsed magnetic treatment. This proposed method can be effective in improving the high-speed steel tool life. The other way is to test performance under magnetic field treatment. Ayhan [18] studies fatigue life of AISI 4140 steel under magnetic field intensities. The fatigue life approximately improved by 20%, when magnetic field intensity is increased.

The above two treatments have common advantages such as green and controllable cost and easy implementation. However, few scholars study the combination of magnetic field and cryogenic treatment and comprehensive analysis of wear is also lacking. Therefore, based on the

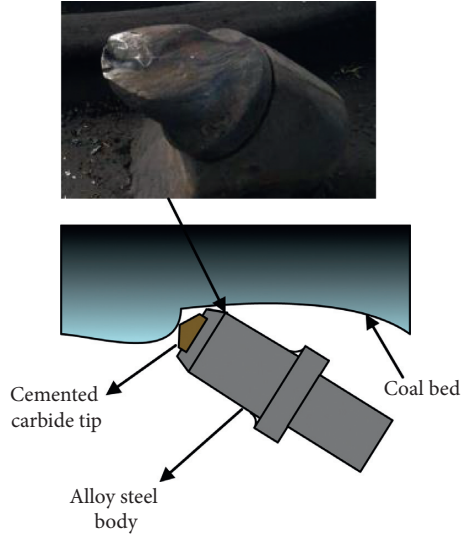


FIGURE 1: Schematic diagram of the conical pick.

failure mode of pick body, this paper applies the magnetic field coupled cryogenic treatment to study the wear resistance of AISI 4140 steel.

2. Materials and Methods

2.1. Preparation of the Materials. AISI 4140 steel ingredient is shown in Table 1. It has high strength, good hardness, and wear resistance, but no obvious temper brittleness. It has been widely used with high fatigue reliability and good load carrying capacity after heat treatment. The test specimen is shown in Figure 2.

2.2. Process Formulation. Conventional heat treatment generally involves quenching and tempering. The researcher has found that the sequence of cryogenic treatment is best between quenching and tempering [19]. This paper was to integrate static magnetic field on the basis of cryogenic treatment. The process was set to four stages: quenching, magnetic field coupled deep cryogenic treatment, low temperature tempering, and medium temperature tempering. Low temperature tempering can effectively resist coarsening of carbide [20]. The specific process setting is shown in Figure 3.

As shown in Figure 3, cryogenic treatment was carried out in cryogenic treatment system by gasification endothermic of liquid nitrogen. The best cryogenic temperature set as 113 K [21]. It belongs to deep cryogenic treatment (113–77 K). The realization of the magnetic field was based on two NdFeB permanent magnets [22]. The magnetic field should be placed in the center of cryogenic treatment system.

After the process setting was determined, it was necessary to design a scientific test program. According to the process setting, there were four process groups in test: untreated group (UT), heat treatment group (HT), deep cryogenic treatment group (DCT) and magnetic field

TABLE 1: Ingredient of AISI 4140 steel (% , mass fraction).

Element	C	Si	Mn	Cr	Mo	P	S	Ni	Fe
Content	0.42	0.25	0.59	1.0	0.17	0.014	0.01	0.03	Balance

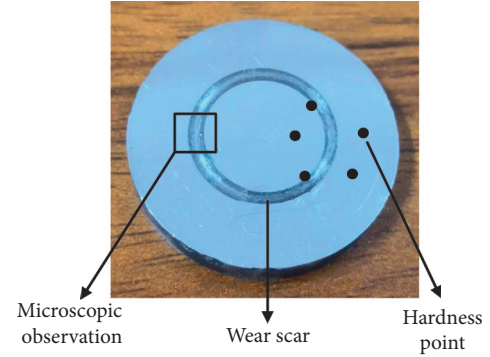


FIGURE 2: Object of specimen.

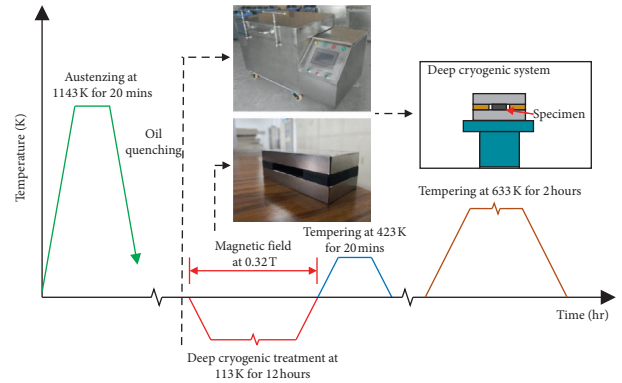


FIGURE 3: Schematic diagram of process setting.

coupled deep cryogenic treatment group (MDCT). The specific process program is shown in Table 2.

2.3. Hardness and Wear Test. Hardness is the ability of a material to resist the pressing of hard objects into its surface. The hardness was measured as a HRC-150A Rockwell hardness tester with a range of 20–70 HRC. Five hardness points were selected near the wear scar (Figure 2).

After the hardness test above, the same specimen can be used for wear resistance test. The wear equipment was the CFT-I material surface wear tester. It also records the dynamic friction coefficient in wear. Based on the tested to better simulate the actual working conditions, the specimen selected the rotary friction. The grinding block material was selected from Si_3N_4 ceramic ball of 5 mm in diameter. The other parameter setting is shown in Table 3 [21]. Before and after wear, the average was m_1 and m_2 , respectively. So, the wear ratio was $(m_1 - m_2) / m_1$.

2.4. Microscopic Observation. The main instruments used in microscopic observation were scanning electron microscope

TABLE 2: Process program.

Group	Quenching	Deep cryogenic treatment	Magnetic field treatment	Tempering
UT	N	N	N	N
HT	Y	N	N	Y
DCT	Y	Y	N	Y
MDCT	Y	Y	Y	Y

“Y” means yes and “N” means no.

TABLE 3: Rotary wear test parameter.

Normal load (N)	Turning radius (mm)	Sliding speed (r/min)	Time (min)
100	7	200	40

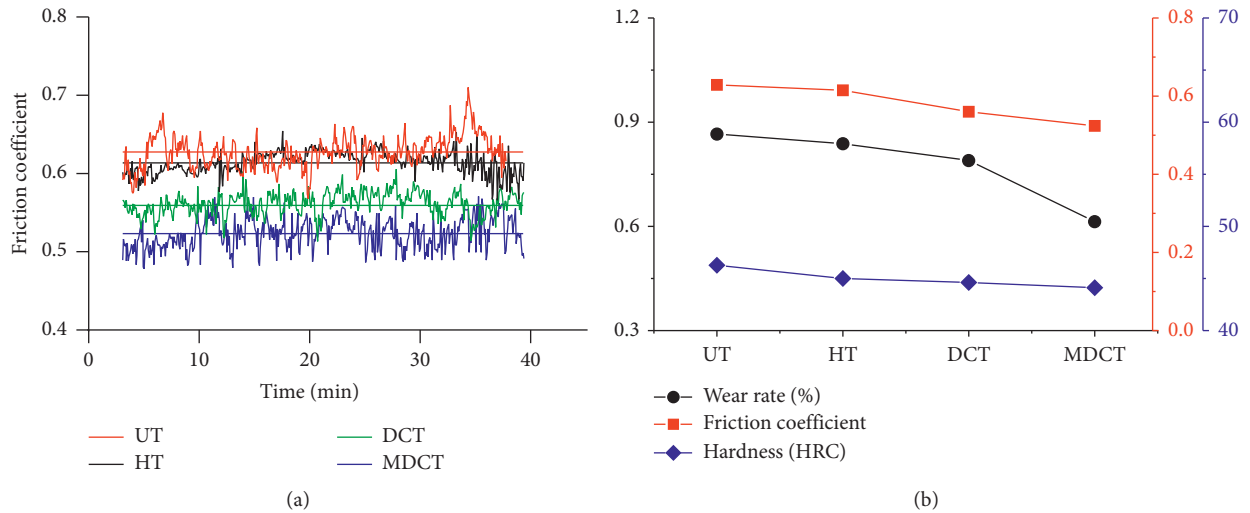


FIGURE 4: Mechanical property of process groups: (a) Dynamic friction coefficient; (b) wear rate, friction coefficient, and hardness.

(SEM) and X-ray diffraction (XRD). Microscopic specimens were taken at the wear scar location (Figure 2). The manufacturer of SEM is VEGA3 SBH from the Czech Republic. The manufacturer of XRD is MiniFlex600 Rigaku from Japan.

3. Results and Discussion

3.1. Mechanical Property. Friction coefficient is an important parameter in tribology, which can reflect the friction surface condition to a certain extent. As shown in Figure 4(a), friction coefficient of process groups tend to be consistent in line spectrum shape. The numerical fluctuation range is small. This means that friction and wear stages are relatively stable. But friction coefficient values of each group are different. It can also be seen that the average friction coefficient decreases from UT about 0.63, HT, DCT to MDCT about 0.52. The maximum reduction rate is 17%. These indicate that MDCT reduces the degree of friction.

Figure 4(b) shows the wear rate, average friction coefficient, and hardness of different process groups. It is found that wear rate is reduced from UT, HT, DCT to MDCT. It indicates that the wear resistance of each group increases in order. Compared with wear resistance of UT, wear resistance

of HT, DCT, and MDCT increases by about 3.2%, 8.8%, and 29%, respectively. Furthermore, the wear rate has the same reduction tendency as the friction coefficient. Hardness has no trend as above. Although the trend is to decrease gradually, the maximum reduction rate is only 4.7%. The values are mainly distributed around 45HRC. So, we can conclude that wear resistance is inversely proportional to friction coefficient but is irrelevant to hardness. Friction coefficient reduction may enhance wear resistance. However, Bowden’s [23] friction theory indicates that the coefficient of friction cannot satisfactorily explain the reason for enhancement of wear resistance. We need to obtain a more sufficient reason through microscopic analysis.

3.2. Microstructure. Figure 5 shows the tempered structure of the specimen by SEM observation. It can be judged in the figure: irregularly shaped grain boundary, white grainy carbide, gray-black ferrite, and white strip tempered troostite. Carbide and ferrite are conventional structure under heat treatment. There are three reasons why the white strip is troostite: the temperature of medium temperature tempering is 633 K; the carbon content is about 0.42%; and the hardness is about 45HRC [24]. In the quenching stage,

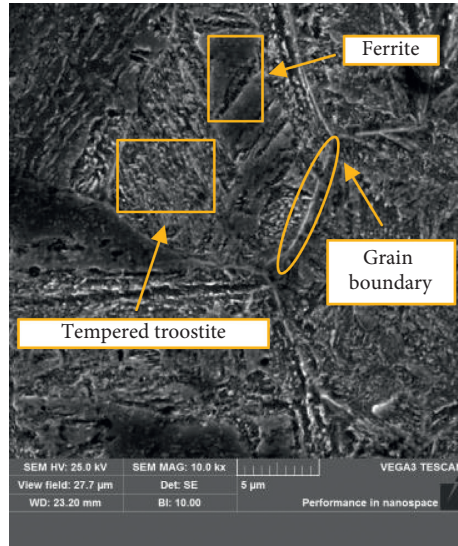
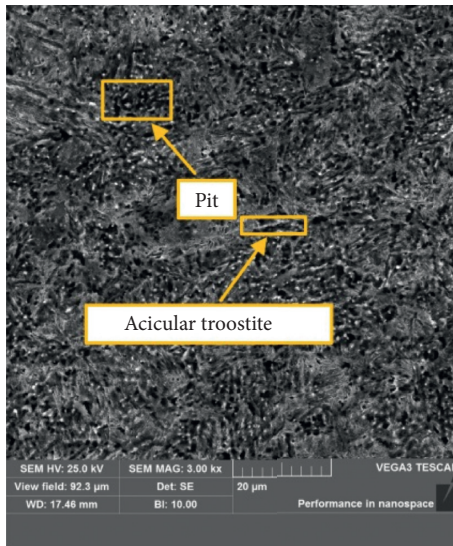
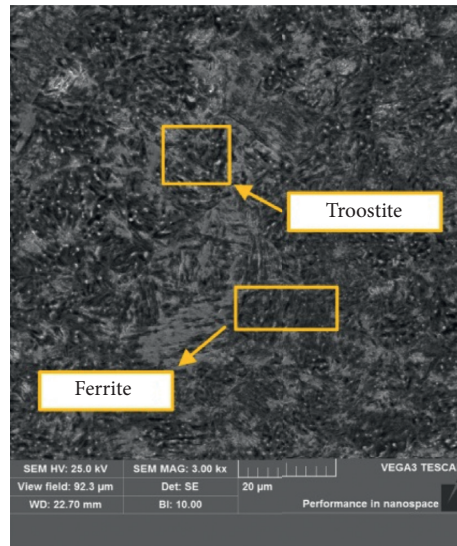


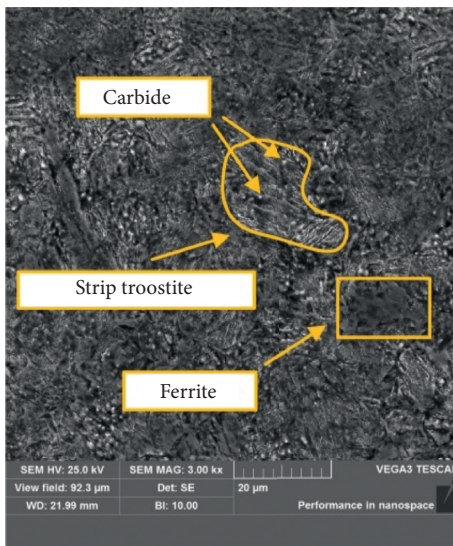
FIGURE 5: SEM image of tempered structure (10.00 kx).



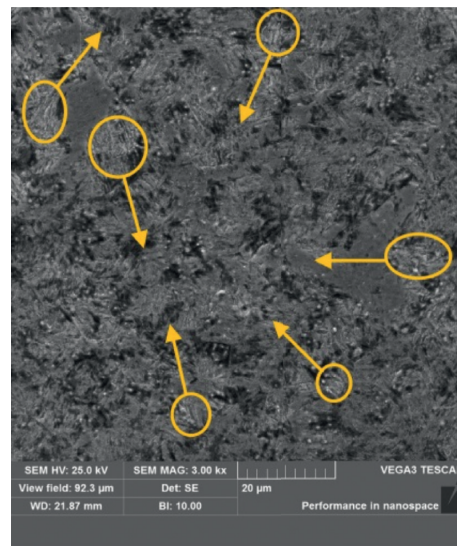
(a)



(b)



(c)



(d)

FIGURE 6: SEM images of process groups (3.00 kx): (a) UT, (b) HT, (c) DCT, (d) MDCT.

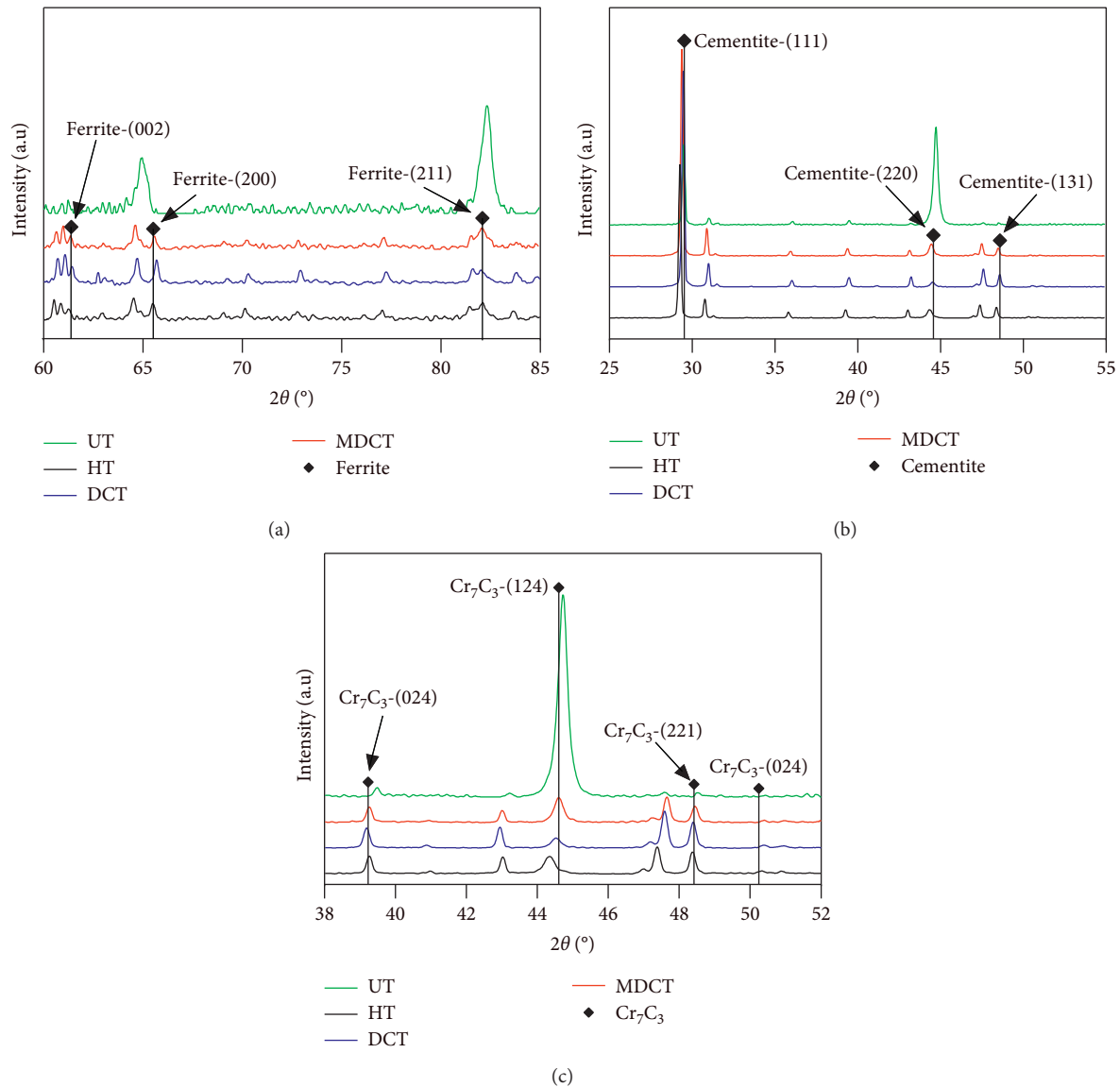


FIGURE 7: XRD pattern of process groups: (a) ferrite, (b) cementite, and (c) Cr_7C_3 .

austenite is transformed into martensite by continuous cooling. During the medium temperature tempering stage, carbon precipitation in martensite begins to aggregate and grow to cementite (Fe_3C). The matrix martensite is restored to ferrite. The two phases are mechanically mixed into tempered troostite. It has high wear resistance, strength, and hardness [25].

3.2.1. Effect of Conventional Heat Treatment. In Figure 6(a), the white troostite has sparse and brittle acicular distribution with many microgaps. White acicular troostite is the least and the distribution is poor. There are many large particle carbide and black honeycomb pit. This characteristic causes uneven force in the wear test. The pit is easily broken by the ceramic ball. These lead to the worst performance on wear resistance. Figure 6(b) shows a little distribution of small granular white carbide and uneven white strip troostite. The

troostite alternately distributes with thin strip ferrite. The quenching promotes the transformation of austenite to martensite, which in turn transforms into troostite in tempering. The pit is also significantly reduced. They prompt a slight increase on wear resistance.

3.2.2. Effect of Deep Cryogenic Treatment. Figure 6(c) shows a quantity of thickness strip troostite and ferrite. A small amount of gaps were distributed on the surface of the material. DCT transforms more troostite and carbide. The reason is that DCT can lower the temperature below M_s (start temperature of martensite transformation) to generate more martensite [26]. The transformed troostite also increased in the later tempering. Carbon accumulates at the martensite boundary to form cementite (Fe_3C) or carbide (Cr_7C_3) [27]. The granular carbide is mostly distributed in discontinuous areas. The result is that the hardness can be

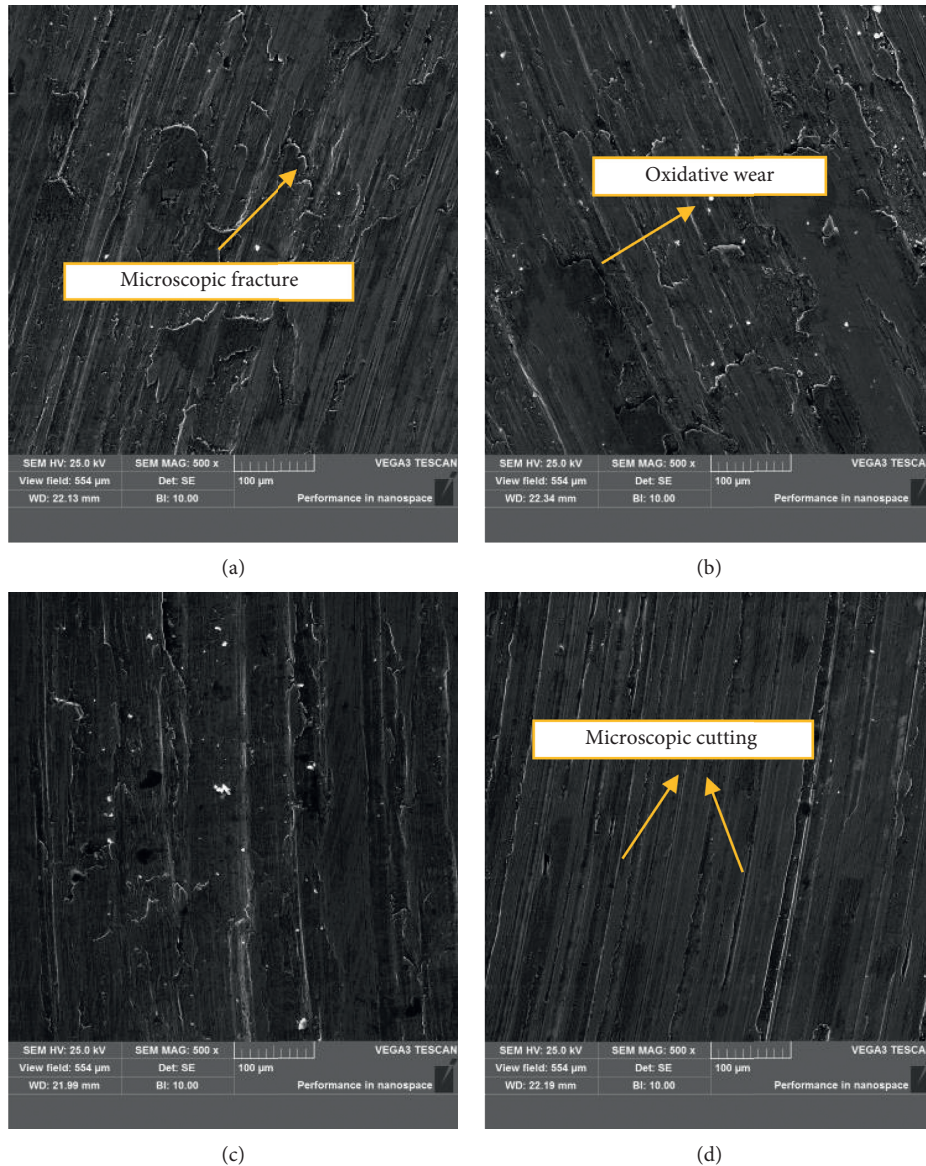


FIGURE 8: SEM images of wear scar on different process surfaces (500x): (a) UT, (b) HT, (c) DCT, and (d) MDCT.

increased. In addition, the matrix martensite is also optimized during the precipitation of carbon. Therefore, the wear resistance of the DCT is greatly enhanced.

3.2.3. Effect of Magnetic Field Coupled Deep Cryogenic Treatment. Figure 6(d) reveals best troostite distribution. The strip troostite is thicker and denser in multidirectional distribution. This indicates that more optimized troostite is produced than in cryogenic treatment. On the basis of the deep cryogenic treatment to lower the temperature, the magnetic field treatment changes Gibbs free energy. This will increase M_s and more easily induce martensite transformation [28, 29]. Besides, the magnetostrictive effect activates flexible dislocation movement in all directions [30]. Multidirectional troostite distribution optimizes surface roughness. So, the treatment eliminates unfavorable gaps and repairs microscopic defect. Dislocation movement can

also break down carbide [31]. The refined carbide strengthens the matrix martensite. These factors make a large amount of troostite to fill material surface. Therefore, the group has the highest wear resistance.

The content of troostite and carbide can also be obtained by XRD analysis. Figures 7(a) and 7(b) show the results of ferrite and cementite, respectively. They are the necessary phases of the composition of the troostite. It can be seen that the peaks of DCT and MDCT are matched, while other processes have large deviations. This shows that a large amount of troostite is produced. In addition, it can be seen from Figure 7(c) that MDCT has the highest carbide content. According to the above analysis, MDCT is the most ideal distribution of troostite and carbide.

3.3. Wear Mechanism. The analysis of wear mechanism is necessary to wear. SEM can observe the surface wear scar of

different groups. Figure 8 shows a clear elongated cutting groove with curvature in four images. In the wear test, the rotary friction motion is performed between the ceramic ball and the specimen. The higher hardness ceramic ball can cause plastic deformation on the surface of specimen. The huge cutting stress pushes the material to both sides. The surface forms many small width and depth cutting grooves with small chips. The wear mechanism is abrasive wear in the form of microscopic cutting [32].

Figures 8(a) and 8(b) have similar wear characteristics. In addition to cutting groove, the surface of specimen presents large delaminated areas and patchy dark areas. When cut depth reaches a critical depth, a large amount of brittle structure is cracked in the wear test. The expansion of the crack and its own unfavorable pit lead to a large delaminated area. The wear mechanism is abrasive wear in the form of microscopic fracture [33]. The dark area made oxidation reaction with friction heat. The surface is subjected to oxidative wear [34]. Therefore, the main wear mechanisms of UT and HT are oxidative wear and abrasive wear in the form of microscopic cutting and microscopic fracture. The result is a higher wear rate in both groups. However, the delaminated area and the black area are significantly reduced in Figure 8(c). The surface has many evenly spaced cutting grooves with few black areas. The wear mechanism is microscopic cutting but little oxidative wear. The reason is that the surface has tempered troostite with high strength and toughness. In Figure 8(d), there are only grooves on the surface. As material property is further enhanced, the cutting stress only pushes the material to both sides without greater damage. Therefore, MDCT is the most satisfactory wear resistance performance. In summary, type and degree of wear are successively reduced from UT, HT, DCT to MDCT.

4. Conclusion

In this study, the effect of magnetic field coupled deep cryogenic treatment on wear resistance of AISI 4140 steel has been investigated. From the mechanical performance testing and microanalysis, the following conclusions have been drawn.

- (1) For AISI 4140 steel, compared with wear resistance of UT, wear resistance of HT, DCT, and MDCT increased by about 3.2%, 8.8%, and 29%, respectively. Besides, wear resistance is inversely proportional to friction coefficient but irrelevant to hardness.
- (2) DCT lowers temperature to generate more martensite. The carbon in martensite precipitates as cementite or carbide. The matrix martensite is also optimized during the precipitation of carbon. The wear resistance of the DCT is greatly enhanced.
- (3) MDCT can raise M_s to generate more martensite. The magnetostrictive effect activates flexible dislocation movement in all directions. This leads to

multidirectional distribution and optimized carbide. The result strengthens material property and repairs surface defects. Based on the cryogenic treatment, the best wear resistance is obtained.

- (4) The mechanism of MDCT is abrasive wear in the form of microscopic cutting, while other process groups are oxidative wear and abrasive wear in the form of microscopic cutting and microscopic fracture.

Data Availability

The data used to support the findings of this study are available from the corresponding author upon request.

Conflicts of Interest

The authors declare that there are no conflicts of interest regarding the publication of this paper.

Acknowledgments

This work was supported by the Natural Science Foundation of China (NSFC) (Grant no. 51275333).

References

- [1] S. Dewangan, S. Chattopadhyaya, and S. Hloch, "Wear assessment of conical pick used in coal cutting operation," *Rock Mechanics and Rock Engineering*, vol. 48, no. 5, pp. 2129–2139, 2015.
- [2] M. Araghchi, H. Mansouri, and R. Vafaei, "Influence of cryogenic thermal treatment on mechanical properties of an Al-Cu-Mg alloy," *Materials Science and Technology*, vol. 34, no. 4, pp. 468–472, 2018.
- [3] A. Molinari, M. Pellizzari, S. Gialanella, G. Straffellini, and K. H. Stiasny, "Effect of deep cryogenic treatment on the mechanical properties of tool steels," *Journal of Materials Processing Technology*, vol. 118, no. 1–3, pp. 350–355, 2001.
- [4] N. A. Özbek, A. Çiçek, M. Gülesin, and O. Özbek, "Effect of cutting conditions on wear performance of cryogenically treated tungsten carbide inserts in dry turning of stainless steel," *Tribology International*, vol. 94, no. 1, pp. 223–233, 2016.
- [5] V. Franco Steier, E. S. Ashiuchi, L. Reißig, and J. A. Araújo, "Effect of a deep cryogenic treatment on wear and microstructure of a 6101 aluminum alloy," *Advances in Materials Science and Engineering*, vol. 2016, Article ID 1582490, 12 pages, 2016.
- [6] S. Li and X. Wu, "Microstructural evolution and corresponding property changes after deep cryotreatment of tool steel," *Materials Science and Technology*, vol. 31, no. 15, pp. 1867–1878, 2015.
- [7] M. Koneshlou, K. Meshinchi Asl, and F. Khomamizadeh, "Effect of cryogenic treatment on microstructure, mechanical and wear behaviors of AISI H13 hot work tool steel," *Cryogenics*, vol. 51, no. 1, pp. 55–61, 2011.
- [8] A. P. Gulyaev, "Improved methods of heat treating high speed steels to improve the cutting properties," *Metallurg*, vol. 12, pp. 65–77, 1937.
- [9] P. Gordon and M. Cohen, "The transformation of retained austenite in high speed steel at sub-atmospheric

- temperatures,” *Transactions of the American Society of Metals*, vol. 30, pp. 569–587, 1942.
- [10] G. B. Berlien, “Sub-Zero hardening cycles,” *Steel*, vol. 1, no. 10, pp. 86–90, 1944.
- [11] M. K. Vidyarthi, A. K. Ghose, and I. Chakrabarty, “Effect of deep cryogenic treatment on the microstructure and wear performance of Cr-Mn-Cu white cast iron grinding media,” *Cryogenics*, vol. 58, pp. 85–92, 2013.
- [12] D. Senthilkumar and I. Rajendran, “Effect of cryogenic treatment on the hardness and tensile behaviour of AISI 4140 steel,” *International Journal of Microstructure and Materials Properties*, vol. 26, no. 2, pp. 366–367, 2011.
- [13] J. J. Soto-Bernal, R. Gonzalez-Mota, I. Rosales-Candelas, and J. A. Ortiz-Lozano, “Effects of static magnetic fields on the physical, mechanical, and microstructural properties of cement pastes,” *Advances in Materials Science and Engineering*, vol. 2015, Article ID 934195, 9 pages, 2015.
- [14] T. Kakeshita, K. Kuroiwa, and K. Shimizu, “Effect of magnetic fields on athermal and isothermal martensitic transformations in Fe-Ni-Mn alloys,” *Materials Transactions, Japan Institute of Metals*, vol. 34, pp. 415–422, 1993.
- [15] Y. Zhang, X. Zhao, N. Bozzolo, C. He, L. Zuo, and C. Esling, “Low Temperature tempering of a medium carbon steel in high magnetic field,” *ISIJ International*, vol. 45, no. 6, pp. 913–917, 2005.
- [16] T. P. Hou, K. M. Wu, and G. He, “Effect of tempering temperature on carbide precipitation behaviours in high strength low alloy steel under high magnetic field,” *Materials Science and Technology*, vol. 30, no. 8, pp. 900–905, 2014.
- [17] L. Ma, W. Zhao, Z. Liang et al., “An investigation on the mechanical property changing mechanism of high speed steel by pulsed magnetic treatment,” *Materials Science and Engineering: A*, vol. 609, pp. 16–25, 2014.
- [18] Ç. Ayhan, Y. A. Fatih, A. Akgün, and K. Mehmet, “Effect of magnetic treatment on fatigue life of AISI 4140 steel,” *Materials & Design*, vol. 26, pp. 700–704, 2005.
- [19] J. Li, X. Yan, X. Liang, H. Guo, and D. Y. Li, “Influence of different cryogenic treatments on high-temperature wear behavior of M2 steel,” *Wear*, vol. 376–377, pp. 1112–1121, 2017.
- [20] M. Pellizzari, “Influence of deep cryogenic treatment on the properties of conventional and PM high speed steels,” *Metallurgia Italiana Impact Factor*, vol. 100, no. 8, pp. 17–22, 2008.
- [21] X. G. Yan and D. Y. Li, “Effects of the sub-zero treatment condition on microstructure, mechanical behavior and wear resistance of W9Mo3Cr4V high speed steel,” *Wear*, vol. 302, no. 1–2, pp. 854–862, 2013.
- [22] A. S. Kim and F. E. Camp, “High performance NdFeB magnets (invited),” *Journal of Applied Physics*, vol. 79, no. 8, p. 5035, 1996.
- [23] F. P. Bowden and D. Tabor, “Friction, lubrication and wear: a survey of work during the last decade,” *British Journal of Applied Physics*, vol. 17, no. 12, pp. 1521–1544, 1966.
- [24] M.-x. Wei, S.-q. Wang, L. Wang, X.-h. Wang, and K.-m. Chen, “Selection of heat treatment process and wear mechanism of high wear resistant cast hot-forging die steel,” *Journal of Iron and Steel Research International*, vol. 19, no. 5, pp. 50–57, 2012.
- [25] S. Q. Wang, M. X. Wei, and Y. T. Zhao, “Effects of the tribo-oxide and matrix on dry sliding wear characteristics and mechanisms of a cast steel,” *Wear*, vol. 269, no. 5–6, pp. 424–434, 2010.
- [26] D. Das, A. K. Dutta, and K. K. Ray, “Optimization of the duration of cryogenic processing to maximize wear resistance of AISI D2 steel,” *Cryogenics*, vol. 49, no. 5, pp. 176–184, 2009.
- [27] S. Li, L. Deng, X. Wu, Y. a. Min, and H. Wang, “Influence of deep cryogenic treatment on microstructure and evaluation by internal friction of a tool steel,” *Cryogenics*, vol. 50, no. 11–12, pp. 754–758, 2010.
- [28] Y. Zhang, N. Gey, C. He, X. Zhao, L. Zuo, and C. Esling, “High temperature tempering behaviors in a structural steel under high magnetic field,” *Acta Materialia*, vol. 52, no. 12, pp. 3467–3474, 2004.
- [29] S. Ken’ichi and K. Tomoyuki, “Effect of magnetic fields on martensitic transformations in ferrous alloys and steels,” *ISIJ International*, vol. 29, pp. 97–116, 1989.
- [30] Q. Shao, J. Kang, Z. Xing et al., “Effect of pulsed magnetic field treatment on the residual stress of 20Cr2Ni4A steel,” *Journal of Magnetism and Magnetic Materials*, vol. 476, pp. 218–224, 2019.
- [31] L. P. Ma, Z. Q. Liang, X. B. Wang, W. X. Zhao, L. Jiao, and Z. B. Liu, “Influence of pulsed magnetic treatment on microstructures and mechanical properties of M42 high speed steel tool,” *Acta Metallurgica Sinica*, vol. 51, no. 3, pp. 307–314, 2015, in Chinese.
- [32] L. Lin, Q. Mao, Y. Xia et al., “Experimental study of specific matching characteristics of tunnel boring machine cutter ring properties and rock,” *Wear*, vol. 378–379, pp. 1–10, 2017.
- [33] X. Zhang, Y. Xia, Y. Zhang et al., “Experimental study on wear behaviors of TBM disc cutter ring under drying, water and seawater conditions,” *Wear*, vol. 392–393, pp. 109–117, 2017.
- [34] S. Q. Wang, L. Wang, Y. T. Zhao, Y. Sun, and Z. R. Yang, “Mild-to-severe wear transition and transition region of oxidative wear in steels,” *Wear*, vol. 306, pp. 311–320, 2017.